Electronic Supplementary Material (ESI) for Environmental Science: Advances.

Supplementary Information: Controlling crystallisation and dissolution of biogenic $CaCO_3$ via dissolved magnesium cations

Toby Morton-Collings,[a] Minjun Yang,[a,b] Richard G. Compton[a*]

[a] Mr T. Morton-Collings, Dr. M. Yang and Prof. R. G. Compton
Physical and Theoretical Chemistry Laboratory, Department of Chemistry,
University of Oxford,
South Parks Road, Oxford, Great Britain
E-mail: Richard.Compton@chem.ox.ac.uk
[b] Dr. M. Yang
Department of Chemistry,
University of Leicester,
University Road, Leicester, Great Britain.

SI Section 1: Crystalisation of $CaCO_3$ on biogenic coccoliths

In the main manuscript images of *C. braarudii* coccoliths in a supersaturated calcite solution ($\Omega_{calcite} = 2200$) in the *absence of any* Mg^{2+} are shown as a function of time following immersion (see Figures 2 a). Video S1, which is available as part of the online Supporting Information, shows a timelapse of the growth of a coccolith and three synthetic calcite particles over an experimental timescale of 100 minutes. The projection area of the biogenic coccolith (solid line) and synthetic $CaCO_3$ particles (dotted lines) was analysed from the timelapse video and plotted as a function of time in Figure S1 a). Qualitatively, the coccolith and pure calcite particles can be seen to grow at similar rates. As discussed in the main text and shown in the wide-angle timelapse video, Video S2, the concomitant nucleation of solid $CaCO_3$ particles in the solution phase prevents quantitative analysis of the rate of growth of the particles of interest due to an overlap of the diffusion layers of neighbouring particles.

Figures S1 b) plots the projection area of two coccoliths (solid lines) and two synthetic calcite particles (dotted lines) as a function of time in a supersaturated calcite solution ($\Omega_{calcite}$ = 2200) containing 5.5 mM Mg^{2+}. Video S3 is a timelapse video showing the particle growth. Similar to Figures S1 a), the growth rate of biogenic coccoliths in 5.5 mM Mg^{2+} is comparable to pure, synthetic calcite particles. As above, interpreting subtle differences in the growth rates between the coccoliths and synthetic particles herein should be approached with caution due to the concomitant nucleation of solid $CaCO_3$ particles in the solution. A wide-angle timelapse video, Video S4, showing particle growth in 5.5 mM of Mg^{2+} is available in the online Supplementary Information. In the timelapse video a fraction of particles can be seen to show characteristic signs of aragonite growth after 60 minutes of the onset of the experiment. Note that the shapes of the $CaCO_3$ particles nucleated in the supersaturated solution are distinctively different with and without Mg^{2+}.

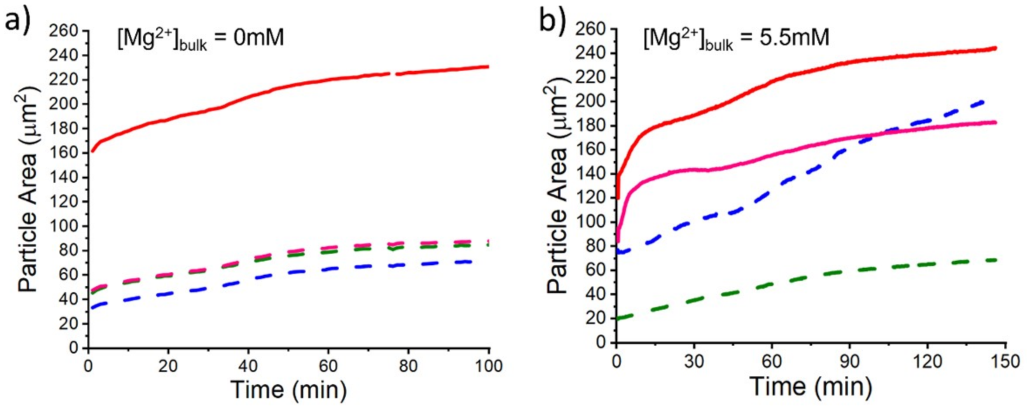

Figure S1. Projection area of biogenic and synthetic $CaCO_3$ particles as a function of time exposed to a solution supersaturated with respect of calcite ($\Omega_{calcite}$ = 2200). ***a)*** *No added Mg^{2+} and* ***b)*** *with 5.5 mM Mg^{2+}. Solid lines: C. braarudii coccoliths. Dotted lines: pure, synthetic calcite particles. The timelapse growth videos of the particles in Figure S1 a) and b) are available in the online Supporting Information as Video S1 and Video S3, respectively.*

The structure of *C. braarudii* coccoliths consists of distal and proximal shields connected through a central opening. [1,2] The coccolith is attached to the coccolithophore with the distal shield facing outwards and proximal shield facing towards the underlying biological cell. Figure S2 shows complementary SEM images of the "underside" of *C. braarudii* coccoliths showing the proximal shield before and after immersion in supersaturated calcite solutions. Figure S2 a) shows two naturally occurring, unmodified coccoliths, the shapes and sizes of which are consistent with those reported elsewhere in the literature[2,3]. Figure S2 b) shows a coccolith after 24 hours immersion in the supersaturated calcite solution ($\Omega_{\text{calcite}} = 2200$) in the *absence of any* Mg^{2+}, which results in additional jagged features on the edges of the proximal and distal shields as compared to the unmodified coccolith. The morphology of these jagged features resembles that of rhombohedral-shaped particles (circled in yellow) nucleated in the solution phase. The crystalline structure of the rhombohedral-shaped calcite particles nucleated in the solution is confirmed by XRD (orange line, Figure 2 I) reported in the main text). In the presence of 5.5 mM of Mg^{2+}, the morphology of the $CaCO_3$ precipitation on the coccolith shown in the SEM image in Figure S2 c) is characteristically different to the shape-edged calcite crystalline structure but, rather, more consistent with the surface of the rod-shaped $CaCO_3$ particles precipitated in the experiment (highlighted in yellow) and which was confirmed to be aragonite via XRD patterns (red line in Figure 2 I, main text). It is interesting to note that $CaCO_3$ does not precipitate onto the central area of the coccolith, either with or without Mg^{2+} present. Likely this is because the central area is functionalised with organic material for the attachment of the coccolith onto the underlying biological cell.

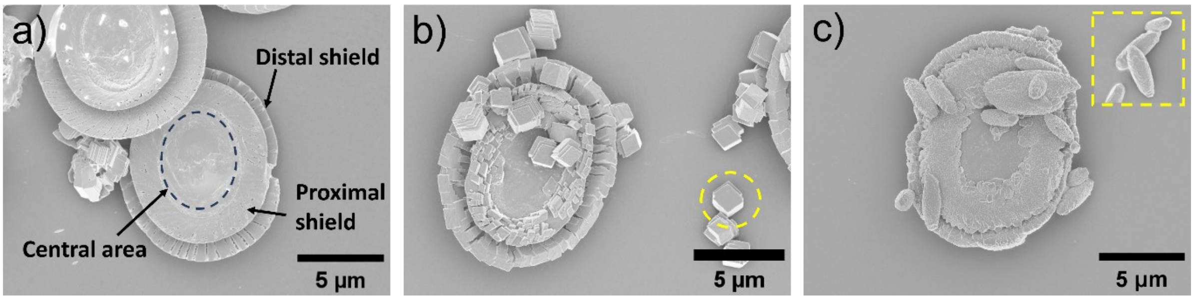

Figure S2. Scanning electron microscope images showing the back of individual C. braarudii coccoliths. ***a)*** *natural coccolith showing no modification.* ***b)*** *after 24 hours in a supersaturated calcite solution, $\Omega_{calcite}$ = 2200.* ***c)*** *after 24 hours immersion in supersaturated calcite solution, $\Omega_{calcite}$ = 2200, with 5.5 mM of Mg^{2+}. The sub-micron sized particles seen on the surface of modified coccoliths in b) and c) are $CaCO_3$ particles precipitated in the supersaturated solution, circled in yellow.*

Figure S3 show SEM images of *C. braarudii* coccospheres with and without artificially induced $CaCO_3$ precipitation. A SEM image of a naturally occurring, unmodified *C. braarudii* coccosphere is shown in Figure S3 a). Note that the term coccosphere refers to the entire $CaCO_3$ exoskeleton, comprising all interlocking coccoliths surrounding the single-cellular organism. Coccospheres, after immersion for 24 hours in the supersaturated calcite solution ($\Omega_{calcite}$ = 2200) in the *absence* of Mg^{2+} and in the *presence* of 5.5 mM Mg^{2+}, are shown in Figure S3 b) and c) respectively. As can be seen, substantial morphological changes can be seen on the distal shields on the individual coccoliths. The features are identical to those seen on coccoliths detached from the coccosphere shown in Figure S2, suggesting coccoliths locked in a coccosphere exhibit similar chemistry to those detached.

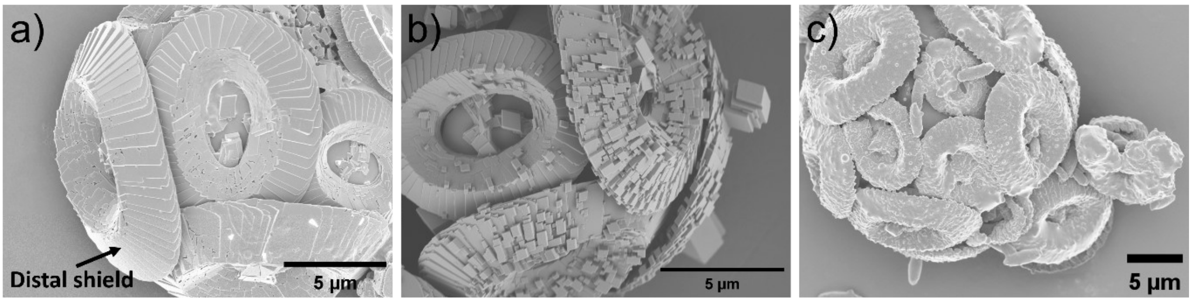

Figure S3. Scanning electron microscope images of individual C. braarudii coccospheres. ***a)*** *natural coccosphere with no modification.* ***b)*** *after 24 hours in a supersaturated calcite solution, $\Omega_{calcite}$ = 2200.* ***c)*** *after 24 hours in a supersaturated calcite solution, $\Omega_{calcite}$ = 2200, and 5.5 mM Mg^{2+}.*

Figure S4 shows an SEM image of two partially intact coccospheres after 24 hours of immersion in a supersaturated calcite solution ($\Omega_{\mathrm{calcite}} = 2200$) *with* 5.5 mM Mg^{2+}. It is interesting to observe that while the surface morphology of the coccoliths is identical to that seen in Figures S2 c) and S3 c), after 24 hours of immersion there is no sign of $CaCO_3$ precipitation on the inner-side of the coccosphere exposed to the supersaturated calcite solution. A likely explanation is that the chemical nature of the organic cellular membrane adjacent to the inner surface of the calcite shell is different to that found on the surface of coccoliths.[4,5]

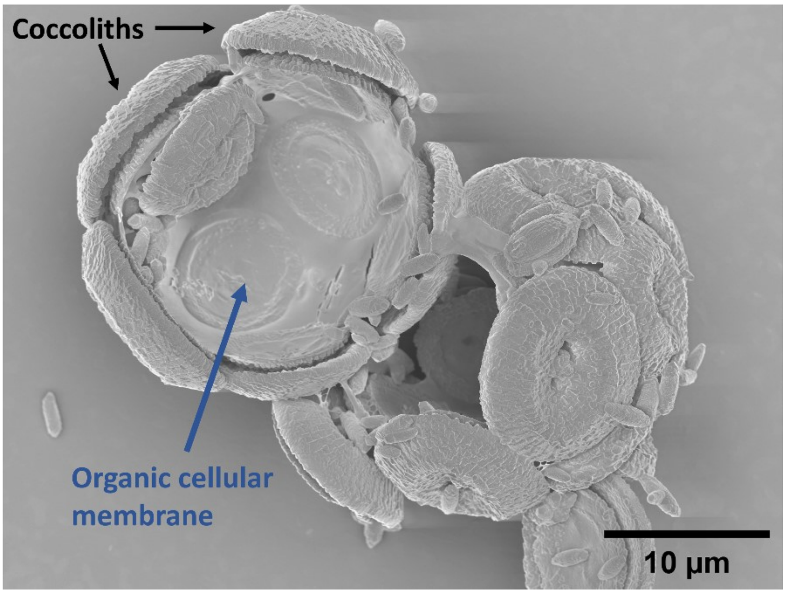

Figure S4. Scanning electron microscope images of two C. braarudii coccospheres after 24 hours in a supersaturated calcite solution, $\Omega_{calcite} = 2200$, *and 5.5 mM* Mg^{2+}.

SI Section 2: Dissolution of biogenic coccoliths

Figure S5 and Figure S6 plot the projection area and effective radius of several individual coccoliths in solutions undersaturated with respect to calcite ($\Omega_{\mathrm{calcite}} = 0$). The concentration of Mg^{2+} in the solution ranged from 0 mM to 100mM with the ionic strength of the solutions maintained at 0.3 M *via* the addition of NaCl. In the absence of Mg^{2+}, coccoliths were seen to completely dissolve after 15 minutes of exposure to the undersaturated aqueous solution. With the addition of Mg^{2+}, a known calcite dissolution inhibitor [6,7], the time required for complete dissolution increases to around 100 minutes. Note that the concentration of Mg^{2+} in seawater is *ca.* 54.6 mM and hence covered by the range of concentrations studied.

The initial rate of coccolith dissolution was obtained by measuring the rate of change in the projected area ($\mu m^2\ s^{-1}$) of the coccoliths between zero and five minutes of dissolution. The yellow shade in Figure S7 shows the region of analysis. Note that the 'dog-leg' transient, explained in author's previous work,[3] are associated with the complete dissolution of the thinnest part of the coccolith resulting in an apparent increase in the rate of recession of the coccolith projected area. This arises because an image of a coccolith, as viewed from the microscope, is projected onto a 2-D plane where the recession in the coccolith thickness does not affect the project area until complete dissolution. Figure S8 plots the average rate of coccolith dissolution ($\mu m^2\ s^{-1}$) as a function of Mg^{2+} concentration. Note that the rates shown in Figure S8 are the average rates of coccolith dissolution as measured between zero and five minutes of dissolution. Overlaid as blue triangles are the equivalent rates of dissolution for pure calcite.[cite ling] The apparent high dissolution rate of the coccolith compared to pure calcite particles is discussed in the main text, where a correction factor of 0.6, based on the coccolith shape-factor as reported by Young *et al.,* was necessary to correct for the intricacy of the shape and morphology of coccoliths compared to a solid calcite particle of the equivalent size.

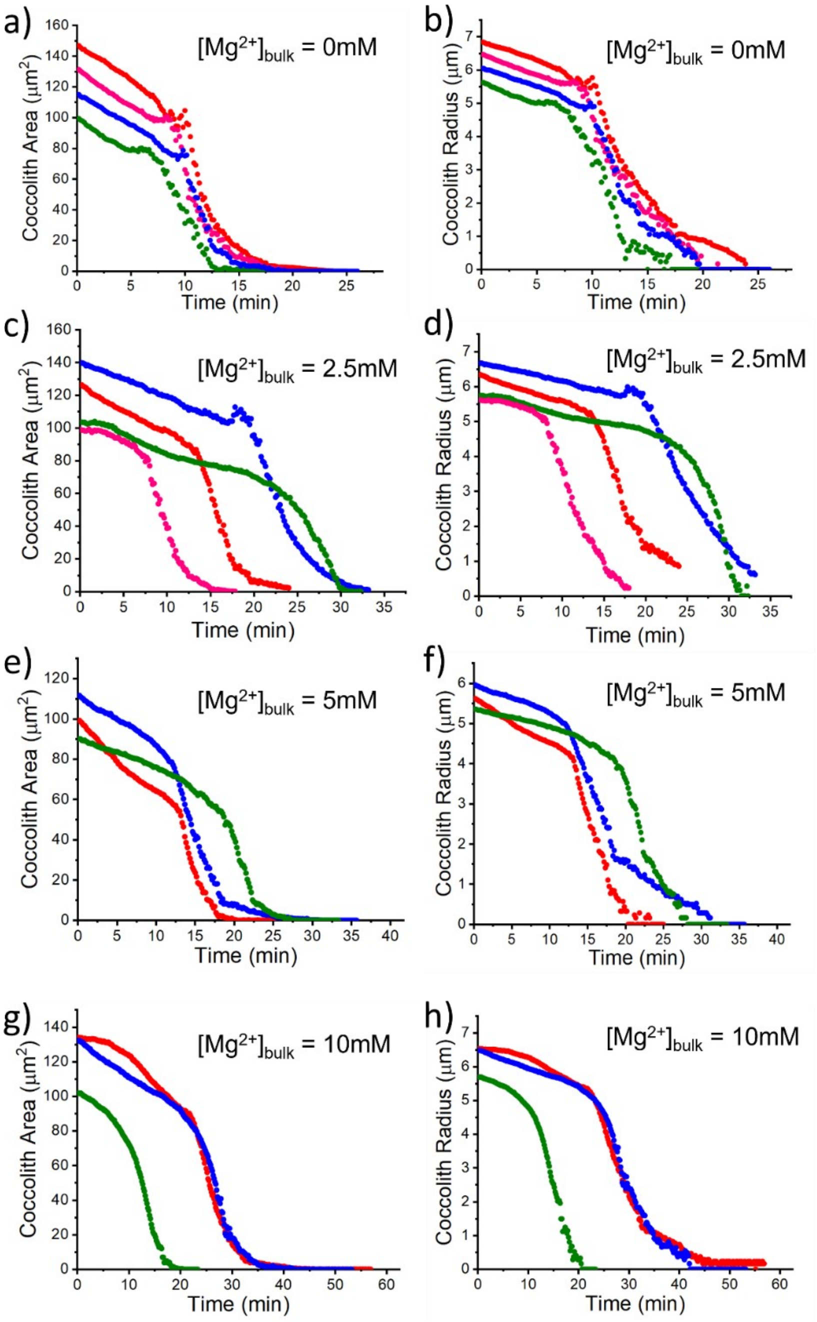

Figure S5. A plot of the temporal evolution in size of C. braarudii coccoliths (projection area and the corresponding effective radius) in undersaturated aqueous solutions with respect to calcite, $\Omega_{calcite} = 0$ *in the presence of* Mg^{2+} *concentrations ranging from 0 mM to 10 mM. The ionic strength of all solutions was fixed at 0.3M via the addition of appropriate amounts of NaCl. The concentrations of* Mg^{2+} *are shown in each of the figures. The calculated effective coccolith radius is derived from the area of a perfect circle (Area =* πr^2*).*

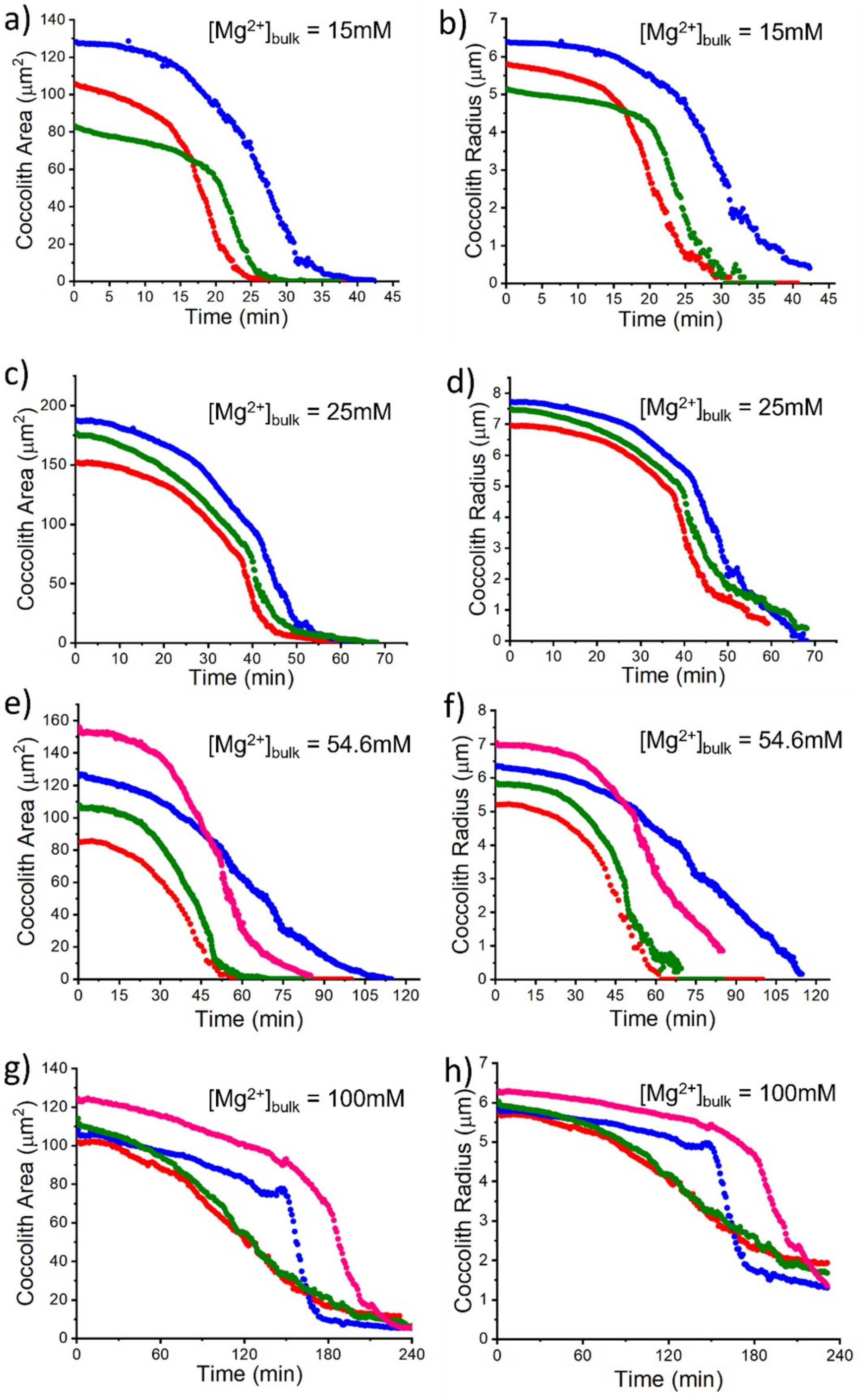

Figure S6. A plot of the temporal evolution in size of C. braarudii coccoliths (projection area and the corresponding effective radius) in undersaturated aqueous solutions with respect to calcite, $\Omega_{calcite} = 0$, in the presence of Mg^{2+} concentrations ranging from 15 mM to 100 mM. The ionic strength of all solutions was fixed at 0.3M via the addition of appropriate amounts of NaCl. The concentrations of Mg^{2+} are shown in each of the figures. The calculated effective coccolith radius is derived from the area of a perfect circle ($Area = \pi r^2$).

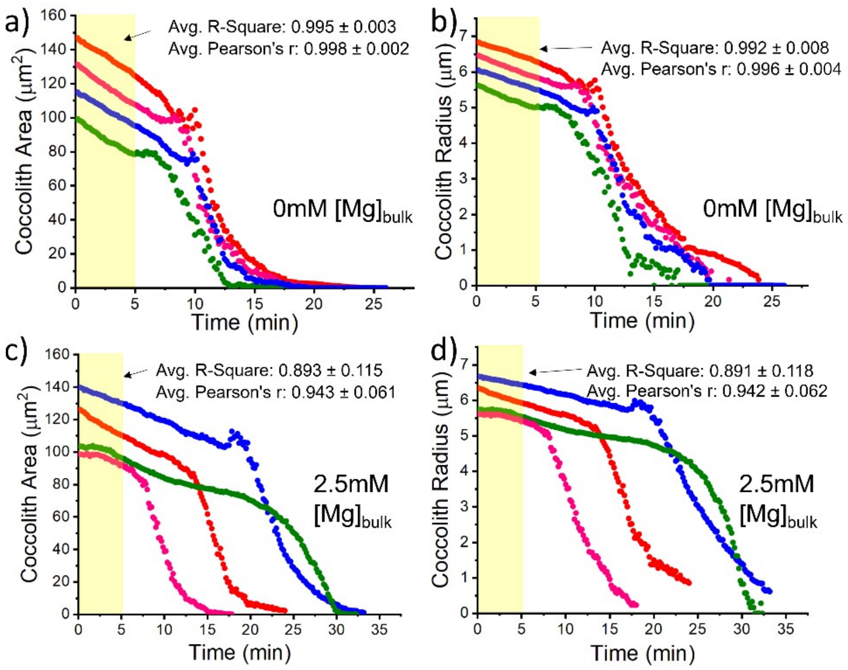

Figure S7. The initial rate of coccolith dissolution is analysed from data recorded over 0 – 5 minutes of the onset of calcite dissolution for all experiments. The yellow shaded region shows the fraction of the data used in the initial rate analysis. The data plotted in a)-d) are the same those in Figure S5 a)-d).

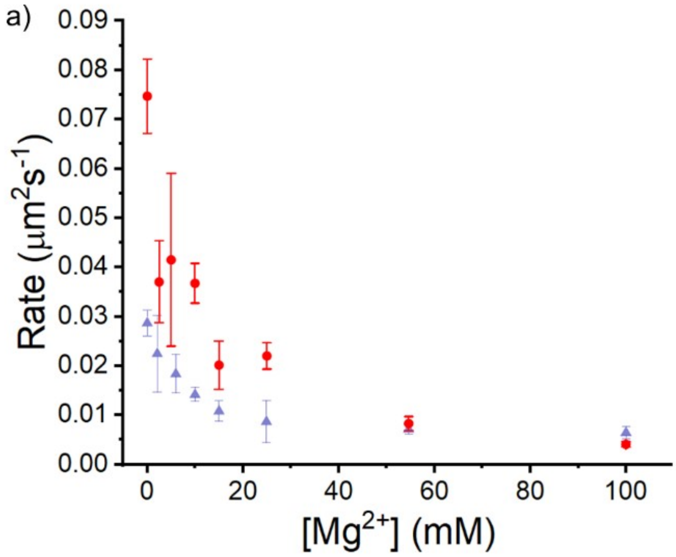

Figure S8. A plot of the initial rate of coccolith dissolution (red circles) as measured without the correction of coccolith shape factor as discussed in the main manuscript. Overlaid as blue triangles are the equivalent rate of dissolution for pure calcite. [8] *Figure 4 c) in the main manuscript shows rate of coccolith dissolution with correction of shape factor.*

Figure S9 shows dark-field optical images of coccoliths after 24 hours immersion in artificial seawater both in the absence of Mg^{2+} and with 54.6 mM of Mg^{2+} present. In both cases, the absence of any $CaCO_3$ precipitation was inferred by the unchanged projection area of the coccoliths observed over 24 hours.

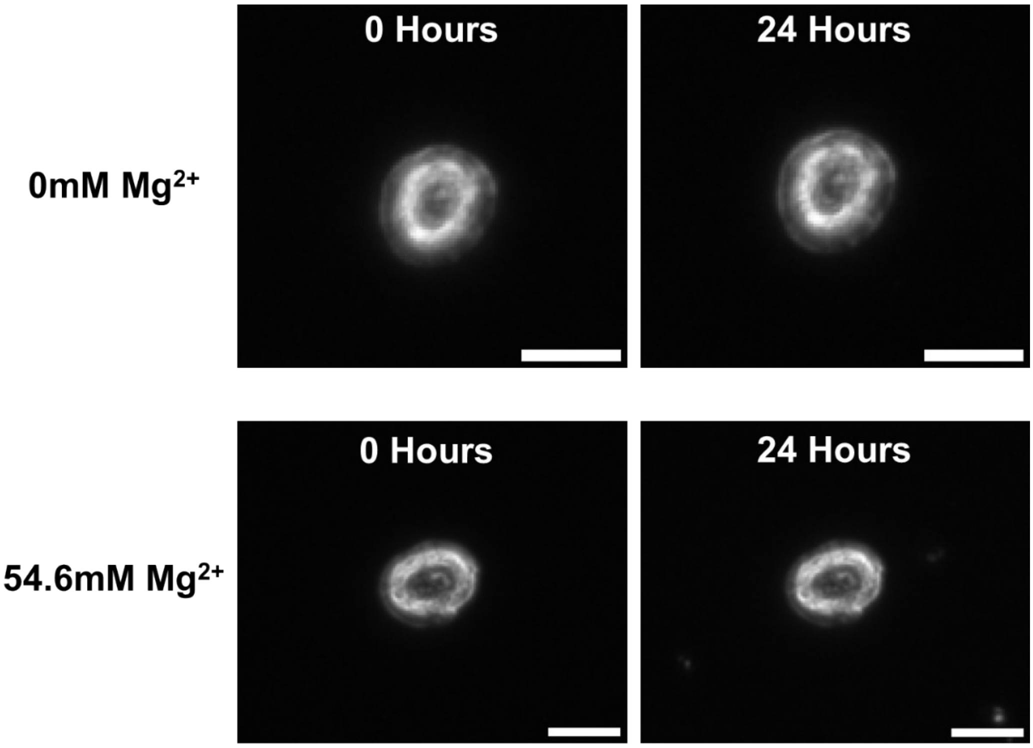

Figure S9. Dark-field microscopy images of coccoliths after 24 hours immersion in artificial seawater in a) absence of any Mg^{2+} *and b) the presence of 54.6 mM of* Mg^{2+}*. Scale bar = 10 µm.*

SI Section 3: Magnesium and Langmuir Adsorption Isotherm

The Langmuir Isotherm for the adsorption of Mg ions on calcite is[9]

$$\theta_{surf} = \frac{[Mg^{2+}]K_{ads}}{1 + [Mg^{2+}]K_{ads}} \qquad \textit{Equation S5}$$

$$(1 - \theta_{surf}) = \frac{1}{1 + [Mg^{2+}]K_{ads}} \qquad \textit{Equation S6}$$

where $K_{Mg^{2+}}$ is the magnesium adsorption equilibrium constant (m^3 mol^{-1}) and θ_{surf} is the fraction of unoccupied sites which scales the rate of dissolution linearly:

$$rate = k_{diss}(1 - \theta_{surf}) = \frac{k_{diss}}{1 + [Mg^{2+}]K_{ads}} \qquad \textit{Equation S7}$$

Therefore:

$$\frac{1}{rate} = \frac{1}{k_{diss}} + \frac{K_{ads}}{k_{diss}}[Mg^{2+}] \qquad \textit{Equation S8}$$

This produces a linear plot when $\frac{1}{rate}$ is plotted as a function of $[Mg^{2+}]$ with gradient $\frac{K_{ads}}{k_{diss}}$ and intercept $\frac{1}{k_{diss}}$.

References

1 Beuvier, T. *et al.* X-ray nanotomography of coccolithophores reveals that coccolith mass and segment number correlate with grid size. *Nature communications* **10**, 751 (2019).

2 Young, J. R. & Henriksen, K. Biomineralization within vesicles: the calcite of coccoliths. *Reviews in mineralogy and geochemistry* **54**, 189-215 (2003).

3 Yang, M. *et al.* Opto‐Electrochemical Dissolution Reveals Coccolith Calcium Carbonate Content. *Angewandte Chemie* **133**, 21167-21174 (2021).

4 Walker, C. E. *et al.* An extracellular polysaccharide-rich organic layer contributes to organization of the coccosphere in coccolithophores. *Frontiers in Marine Science*, 306 (2018).

5 Godoi, R. H. M. *et al.* Organic surface coating on Coccolithophores-Emiliania huxleyi: Its determination and implication in the marine carbon cycle. *Microchemical Journal* **91**, 266-271 (2009).

6 Millero, F. J. The marine inorganic carbon cycle. *Chemical reviews* **107**, 308-341 (2007).

7 Morse, J. W., Arvidson, R. S. & Lüttge, A. Calcium carbonate formation and dissolution. *Chemical reviews* **107**, 342-381 (2007).

8 Yang, M., Tan, L., Batchelor-McAuley, C. & Compton, R. G. *The solubility product controls the rate of calcite dissolution in pure water and seawater* (2023).

9 Atkins, P. *Shriver and Atkins' inorganic chemistry*. (Oxford University Press, USA, 2010).